Dental Materials 40 (2024) 1753–1761

Contents lists available at ScienceDirect

Dental Materials

journal homepage: www.elsevier.com/locate/dental

Direct ink writing with dental composites: A paradigm shift toward sustainable chair-side production

Po-Chun Tseng [a,*], Dar-Bin Shieh [b,c,d], Andreas Kessler [a,f], Dalia Kaisarly [a], Peter Rösch [e], Karl-Heinz Kunzelmann [a]

[a] Department of Conservative Dentistry and Periodontology, University Hospital, LMU Munich, Munich, Germany
[b] School of Dentistry and Institute of Oral Medicine, National Cheng Kung University, Tainan, Taiwan
[c] Center of Applied Nanomedicine and Core Facility Center, National Cheng Kung University, Tainan, Taiwan
[d] Department of Stomatology, National Cheng Kung University Hospital, Tainan, Taiwan
[e] Faculty of Computer Science, Technical University of Applied Sciences, Augsburg, Germany
[f] Department of Prosthetic Dentistry, Faculty of Medicine, Center for Dental Medicine, Medical Center-University of Freiburg, Freiburg, Germany

ARTICLE INFO

Keywords:
Direct ink writing
3D printing
Additive manufacturing
Resin composites
Accuracy

ABSTRACT

Objectives: To evaluate the dimensional accuracy of occlusal veneers printed using a novel direct ink writing (DIW) system and a clinically approved dental composite.

Methods: A novel three-dimensional printer was developed based on the extrusion-based DIW principle. The printer, constructed primarily with open-source hardware, was calibrated to print with a flowable resin composite (Beautifil Flow Plus). The feasibility of this technology was assessed through an evaluation of the dimensional accuracy of 20 printed occlusal veneers using a laboratory confocal scanner. The precision was determined by pairwise superimposition of the 20 prints, resulting in a set of 190 deviation maps used to evaluate between-sample variations.

Results: Without material waste or residuals, the DIW system can print a solid occlusal veneer of a maxillary molar within a 20-minute timeframe. Across all the sampled surface points, the overall unsigned dimensional deviation was 30.1 ± 20.2 µm (mean ± standard deviation), with a median of 24.4 µm (interquartile range of 22.5 µm) and a root mean square value of 36.3 µm. The pairwise superimposition procedure revealed a mean between-sample dimensional deviation of 26.7 ± 4.5 µm (mean ± standard deviation; $n = 190$ pairs), indicating adequate precision. Visualization of the deviation together with the nonextrusion movements highlights the correlation between high-deviation regions and material stringing.

Significance: This study underscores the potential of using the proposed DIW system to create indirect restorations utilizing clinically approved flowable resin composites. Future optimization holds promise for enhancing the printing accuracy and increasing the printing speed.

1. Introduction

Composite resin restorations have become a viable treatment modality in various clinical scenarios. Direct resin composites have proven to be consistently successful in the complete rehabilitation of severely worn teeth [1,2]. However, extensive defects remain challenging, mainly due to the complexity of achieving ideal occlusions and contours [3]. Moreover, the stress generated during the polymerization of bulk resin composites poses a threat to the bonding interface, potentially compromising clinical longevity [4,5]. Indirect restorations are options for the treatment of extensive defects to reduce the level of skill and time required to perform layering while still achieving optimal results.

Despite the clear advantages of indirect restorations, there are still significant disadvantages to traditional laboratory fabrication, such as high costs and additional visits. In response to these challenges, computer-aided manufacturing (CAM) systems have been introduced to dentistry. Shaping can be achieved through subtractive or additive approaches. Although subtractive systems have long demonstrated clinical success, they are linked to significant material waste, tool attrition, initial investments, and high production costs [6,7]. Consequently, researchers are turning their attention to additive manufacturing (AM) for enhanced sustainability and affordability in dental applications [7,8].

* Correspondence to: Department of Conservative Dentistry and Periodontology, University Hospital, LMU Munich, Goethestr. 70, 80336 Munich, Germany.
E-mail address: P.Tseng@campus.lmu.de (P.-C. Tseng).

https://doi.org/10.1016/j.dental.2024.08.002
Received 3 February 2024; Accepted 1 August 2024
Available online 7 August 2024

Additive manufacturing, or three-dimensional (3D) printing, has excellent potential to reduce material waste and lower production costs. Most research and innovations in restorative dentistry currently rely on vat photopolymerization techniques [9]. In these techniques, 3D objects are created by selectively casting polymerizing light onto resin reservoirs. While this approach is utilized in the fabrication of resin-based restorations, it is compatible only with resins with low filler contents due to viscosity constraints [10]. This limitation, in turn, restricts the mechanical properties of printed objects. In addition, after printing, the meticulous postprocessing of printed objects is needed, which includes removal of the residual resin from the object surface using organic solvents and postcuring to improve the mechanical properties of the objects [9]. This cleaning process may inadvertently release hazardous chemicals into the environment and expose dental professionals to ultrafine particles [11,12]. This raises concerns about the potential allergenicity and toxicity of these substances [13].

In this paper, an innovative direct-ink writing (DIW) technology is proposed to overcome the limitations associated with existing techniques. DIW precisely deposits controlled amounts of high-viscosity materials through an extrusion process [14], so highly filled materials can be used for the production of mechanically robust definitive restorations. In particular, this approach reduces occupational exposure to resin chemicals and minimizes the environmental impact by producing virtually no byproducts [15,16]. The recent expiration of patents for DIW technology has made DIW a cost-effective way of producing durable and sustainable indirect restorations [17].

Despite the advantages of the DIW technique, its application in restorative dentistry remains largely unexplored. To support the on-demand production of indirect restorations, we developed a DIW AM system capable of printing with a flowable dental composite. Continuous blue-light illumination was incorporated to solidify the extruded resin composite, preventing material slumping and enabling high-fidelity printing for definitive restorations [18,19]. The DIW approach eliminates the need for postprocessing and machine cleaning, resulting in an efficient and environmentally friendly fabrication process [15]. In addition, we utilized clinically approved material for posterior restorations to minimize the gap to chairside applications. As a pioneering use of DIW for dental composites, the proposed method provides a new avenue for the sustainable and point-of-care production of definitive restorations.

The primary objective of this study was to design and optimize a novel DIW system tailored to printing with a flowable composite. Rigorous assessments of dimensional accuracy were conducted to ensure the system's reliability and clinical feasibility. Moreover, our printer design is accessible to the research community via the Open Science Framework repository, further fostering cross-border collaborations toward affordable indirect restorations [20].

2. Materials and methods

2.1. Machine settings

An experimental 3D printing system was developed based on the DIW principle. The printer builds 3D structures layer by layer using an extruder (Preeflow® eco-PEN 300, ViscoTec, Töging am Inn, Germany) and a nozzle with an interior diameter of 340 μm (Micron-S dispensing tip, Vieweg, Kranzberg, Germany). During printing, the extruder moves only vertically, and the sample platform moves horizontally based on CoreXY kinematics [21]. To gain direct control over the printing process, the extruder's proprietary motor was replaced by a standard stepper motor. The printer was operated with an Arduino Mega 2560 microcontroller and a RAMPS 1.4 extension board, allowing precise optimization of the printing parameters. Furthermore, two blue-light light-emitting diode (LED) modules (DO-BDL 8W-2A, Osram, Regensburg, Germany) were integrated to provide concurrent light-initiated polymerization. This feature ensured rapid solidification of the composite material and reduced slumping during the printing process. The design of the printer is available at https://doi.org/10.17605/OSF.IO/K2Z5S.

2.2. Tuning process

The DIW printing system was calibrated for the precise extrusion of a flowable dental composite (Beautifil Flow Plus F00A3, lot 052178, Shofu, Inc., Kyoto, Japan). Consisting of Bis-GMA, TEGDM, and a filler load of 47 % by volume [22], the composite can also be used for posterior restorations. The tuning process focused on determining the optimal step rate and extrusion volume. Furthermore, continuous blue-light irradiation was applied while ensuring no clogging of the nozzle. All the printed samples were thinly powdered and characterized using a chromatic confocal scanner (KF-30, Syndicad Ingenieurbüro, Munich, Germany) with a scanning resolution of 20 μm in the horizontal direction and an accuracy of 1.5 μm in the vertical direction.

The cross-sectional area of the printed lines was measured to assess the flow of the composite material through the nozzle to ensure consistent and uniform flow. Further adjustments to the printing parameters were made based on the dimensions and flatness of the printed cylinders. Through iterative refinement, scaling factors of 1.5 % in the y-direction and 1 % in the x-direction were established to compensate for polymerization shrinkage.

2.3. Printing and deviation characterization

The occlusal surface of a maxillary first molar model was sliced to generate G-code using Ultimaker Cura (version 5.0.0) with a layer thickness of 100 μm and 100 % infill. The object was constructed layer-by-layer in a sequence of increasing heights, with the infill printed before the respective outer walls within each enclosed region. Since the structure was solid with a flat bottom, no supplementary support structures were required for this investigation. The printed occlusal veneers were postcured for 20 s immediately after printing using a dental light-curing unit (Bluephase style, Ivoclar Vivadent, Schaan, Liechtenstein) with an output exceeding 1000 mW/cm^2. After 24 h, the restorations ($n = 20$) were finely powdered and digitized using the KF-30 scanner.

The 3D scans were imported into ImageJ software as height maps, where the gray value of each pixel represented the vertical height. To mitigate speckle noise resulting from specular reflection, pixels exhibiting white noise were selectively processed using a median filter. The raster images were then saved in TIFF format for subsequent 3D analysis.

For deviation calculations, the images were imported into the open-source software CloudCompare (version 2.12.4) as individual 3D point clouds. The clouds were first roughly aligned with the reference mesh and then registered to the reference using the iterative closest point algorithm without a scaling operation [23]. The deviation of the registered clouds from the reference was computed using the cloud-to-cloud distance algorithm [24]. Data from the lowest layer (less than 100 μm in height) were cropped and removed to reduce measurement inaccuracies in steeply inclined regions [25].

Accuracy consists of trueness and precision. Trueness reflects the extent to which the measured objects deviate from designated dimensions, as defined in the reference model. To assess trueness, the cloud-to-cloud distances between the virtual reference model and each sample were used to create trueness maps (Fig. 1a). Additionally, precision reflects the closeness between two independent samples (Fig. 1d) [26]. Consequently, 190 nonrepetitive pairs were derived from the 2-combinations of the 20 samples. For each pair, the point clouds were aligned to one another, a process also referred to as pairwise superimposition. The cloud-to-cloud distances between the two aligned clouds were subsequently computed to produce precision maps.

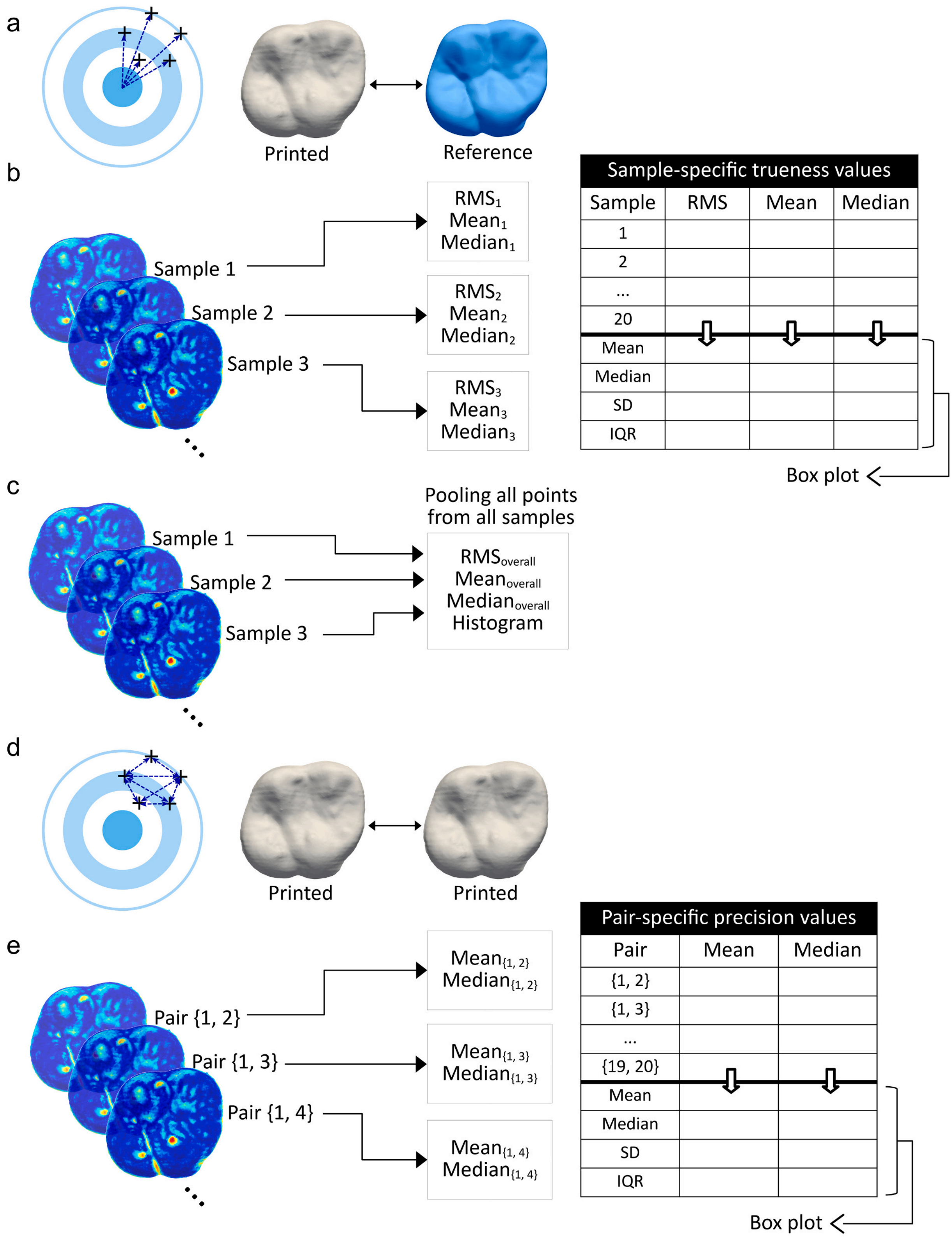

Fig. 1. Schematics illustrating the computation of accuracy in this study. Three sets of statistics are provided to define sample-specific trueness, overall trueness, and pair-specific precision. (a) The trueness is derived from the dimensional deviation of the samples from the reference model. (b) In the conventional approach, deviation data for each sample are preprocessed via arithmetic aggregation operations, generating sample-specific trueness for subsequent statistical analysis. However, in the aggregation process, all within-sample spatial variability is eliminated. (c) To incorporate within-sample deviation variability into the analysis, the surface-wide deviation data for all samples are pooled together to obtain an overall histogram and statistics. This approach provides an efficient and comprehensive overview of the range of deviation across all surfaces. (d) Precision illustrates the differences between each pair of samples. Notably, the 20 samples are superimposed in a pairwise manner, leading to 190 deviation maps. (e) The pair-specific precision is derived through aggregation operations on the deviation maps, similar to preprocessing for sample-specific trueness. RMS: root mean square, SD: standard deviation, IQR: interquartile range.

2.4. Accuracy statistics and visualization

The collected data were statistically analyzed using the software R (version 4.0.2). For trueness evaluation, the sample-specific means and medians of the deviations were derived by preprocessing surface-wide deviation data on a per-sample basis for subsequent statistical analysis (Fig. 1b). The root mean square (RMS) values of the data were presented as a measure of accuracy [27]. Considering that the preprocessing procedure eliminated within-sample spatial variability, additional statistics were provided based on pooled surface-wide deviation data from all samples (Fig. 1c), thereby incorporating spatial components of variability into the analysis.

To assess precision across multiple samples, pair-specific arithmetic means and medians were computed for each deviation map generated by pairwise superimposition ($n = 190$ pairs; Fig. 1e). The sample-specific trueness and pair-specific precision were then summarized in a box plot, providing an overview of the dimensional accuracy metrics at the sample level. Furthermore, the pooled data are presented in a histogram to illustrate their overall statistical distribution.

Statistics alone provide no information on the spatial distribution of the deviation. For visualization, a surface was reconstructed based on a representative sample using the Poisson surface reconstruction algorithm. The previously derived dimensional deviation for a given cloud was mapped to the reconstructed surface to obtain a 3D deviation heat map. As high deviation points were concentrated in certain areas, the G-codes were analyzed to determine what was occurring in those regions. In particular, nonextrusion movements of the extruder were extracted from the G-codes and superimposed on the deviation heat map to help explain the deviation pattern.

3. Results

3.1. Machine cost and production speed

The hardware cost for the DIW printing system was less than 5000 euros. No costs were incurred for the software, as open-source software was used. Personnel costs were not accounted for (Fig. 2a). The system demonstrated that it is capable of printing an occlusal veneer in a time frame of 20 min (Fig. 2b). Notably, the printing process produced minimal material waste because only the required quantities of resin composites were extruded and residue was mitigated. The efficient use of materials contributes to the sustainability and cost efficiency of the printing process.

3.2. Accuracy evaluation

The dimensional accuracy of the printed occlusal veneers was quantitatively evaluated, and the results are summarized in Table 1. As illustrated in Fig. 1, three sets of statistics were provided to assess trueness and precision.

A common approach to analyzing data from multiple samples is to arithmetically preprocess the surface-wide deviation data at the sample level, yielding aggregated sample-specific accuracy metrics for subsequent statistics. A box plot (Fig. 3a) was created to present the sample-specific RMS, mean, and median of the dimensional deviations, with these aggregated metrics illustrated across all samples ($n = 20$). The results indicate a high level of consistency among samples, as evidenced by the minimal variability in terms of sample-specific trueness.

In the second analysis, surface-wide deviation data from all samples were pooled together to include within-sample spatial variability for the overall statistics. The mean dimensional deviation was 30.1 ± 20.2 µm (mean $\pm$ SD), with an RMS of 36.3 µm. The median deviation was 24.4 µm, and the IQR was 22.5 µm. As shown in the histogram (Fig. 3b), the distribution is slightly positively skewed, demonstrating an elongated tail on the right side of the distribution.

For precision, the dimensional deviation between every combination of the two prints was computed through pairwise superimposition and pair-specific aggregation. The mean deviation was 26.7 ± 4.5 µm (mean $\pm$ SD), while the median was 22.6 ± 2.9 µm (mean $\pm$ SD). More detailed statistics are shown in Table 1. The precision values suggest

Table 1
Accuracy statistics.

Sample-Specific Trueness			
Metrics	Mean (SD)	Median (IQR)	95th Percentile
RMS	36.2 (2.6)	35.9 (4.0)	39.3
Mean	30.1 (1.9)	29.9 (3.1)	32.3
Median	24.5 (1.3)	24.2 (1.7)	26.1
Pooled Overall Trueness			
RMS	Mean (SD)	Median (IQR)	95th Percentile
36.3	30.1 (20.2)	24.4 (22.5)	70.5
Precision by Pairwise Superimposition			
Metrics	Mean (SD)	Median (IQR)	95th Percentile
Mean	26.7 (4.5)	25.3 (8.7)	34.2
Median	22.6 (2.9)	21.7 (5.0)	27.5

Units are in µm. RMS: root mean square, SD: standard deviation, IQR: interquartile range.

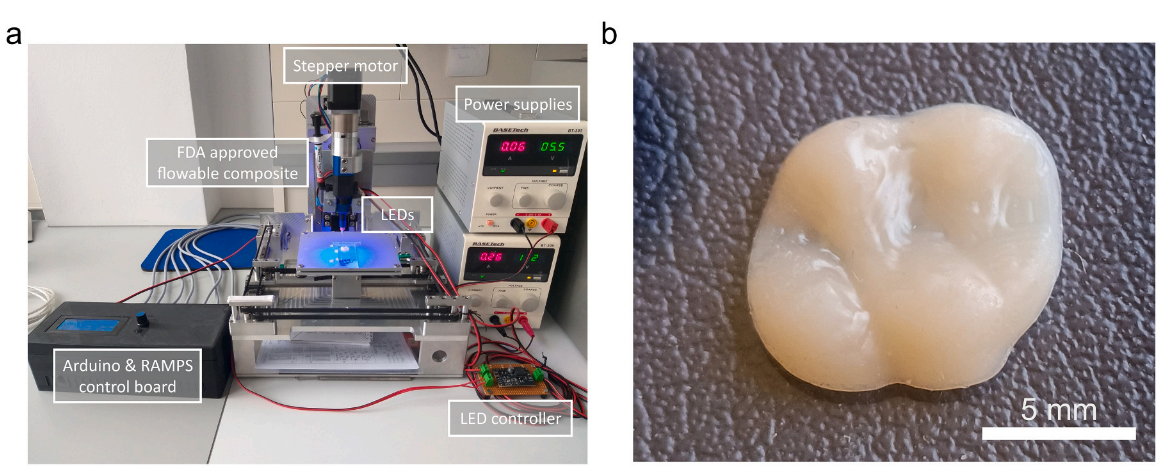

Fig. 2. Machine settings for the 3D printer and a printed occlusal veneer. (a) The printer is built primarily using open-source hardware components. The extruder moves only in the vertical direction to reduce vibration caused by the movement of relatively heavy parts. Blue-light LEDs are installed to provide instantaneous polymerization. (b) The occlusal veneer can be printed within 20 min using a clinically approved flowable composite.

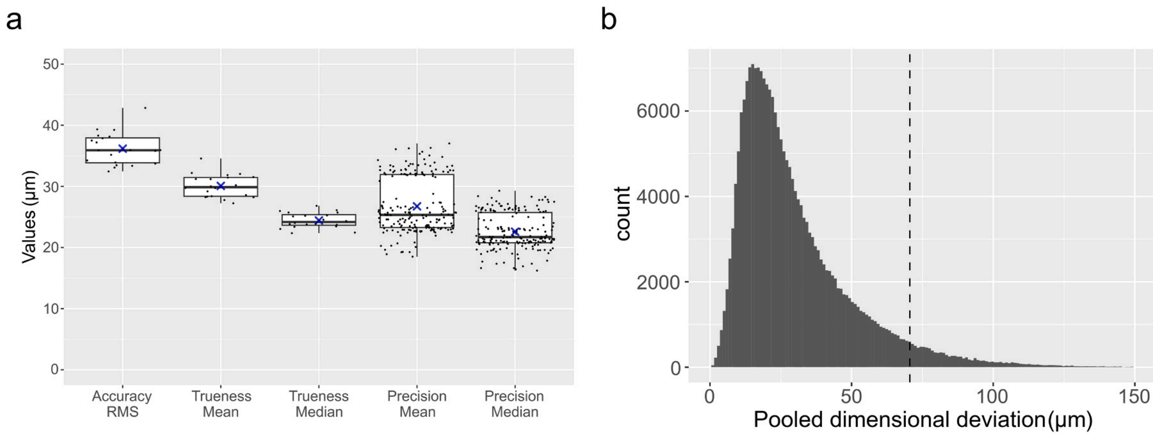

Fig. 3. Box plot of the accuracy metrics and histogram of the overall deviation. (a) Box plots of sample-specific trueness (n = 20) and pair-specific precision (n = 190 pairs). The deviation data are first preprocessed at the sample or pair level using the root mean square (RMS), mean, or median values. The mean values of the boxes are denoted by blue crosses. (b) Histogram illustrating the overall dimensional deviation of all the sampled surfaces. To retain the within-sample spatial variability of deviation, the raw data are pooled without aggregation preprocessing. The dashed line indicates the location of the 95th percentile.

sufficient reproducibility among prints. These precision metrics, also depicted in the box plot (Fig. 3a), provide information on the extent of between-sample variability among the restorations.

3.3. Visualization of deviations

In addition to the statistical distribution and metrics of the dimensional deviation, the spatial distribution of the deviation was visualized for a representative sample. The reference model (Fig. 4a) is presented along with the representative sample (Fig. 4b). As shown in the deviation map (Fig. 4c), the regions of high deviation are concentrated at the palatal groove and several excessive protuberances on the cusps, thus contributing to the positive skewness in the histograms (Fig. 3b and Fig. 4d).

To determine the cause of the protuberances, the nonextrusion movements of the extruder were extracted from the G-codes and superimposed on the deviation map. As shown in Fig. 4e, regions with high deviations were located primarily above the sites where the extruder moved across the outer walls of one printed region to approach the next printing region. Thus, the inaccurate protuberances were likely caused by material "stringing" at the "perimeter-crossing" sites (Fig. 4f).[1]

4. Discussion

In this study, the potential of using DIW technology for the on-demand fabrication of indirect resin composite restorations is demonstrated. While ceramics are generally more wear resistant than resin composites, the latter remain attractive alternatives because of their ease of repair and replacement [28]. The experimental printer demonstrated the capability to produce a posterior veneer within 20 min, with high dimensional accuracy. By further optimizing and mass-producing the system, higher printing speeds and lower machine costs could be achieved. To our knowledge, this study represents the first application of DIW technology in producing composite resin restorations. By utilizing clinically approved materials and open hardware, our approach aims to make indirect restorations affordable and accessible to a wide range of patients.

Despite the global trend of decreased incidence of caries, an increasing demand for indirect restorations is expected in an aging society. A systematic review suggested that approximately 17 % of adults may have severe tooth wear by the age of 70 [29]. If left untreated, damage can lead to problems such as dentin exposure, hypersensitivity, and even alterations to occlusion. Ensuring affordable access to high-quality indirect restorations will be critical to overcome this emerging challenge.

In addition to addressing unmet needs, the DIW system was developed with a particular focus on sustainability, considering environmental, economic, and social factors. To ensure sustainable prosperity for both humanity and the planet, the United Nations has outlined seventeen Sustainable Development Goals (SDGs) in their 2030 Agenda [30]. Nevertheless, these sustainability concepts have yet to be fully integrated into dental practice [31].

This study represents a pivotal step toward more sustainable restorative dentistry. From an environmental perspective, the DIW approach reduces residual resin waste and improves the management of hazardous chemicals. The point-of-care DIW system will contribute to reducing the carbon footprint associated with transportation between dental clinics and laboratories [32]. In addition, the overall cost of the system can be significantly reduced through mass-production and further adoption of open-hardware components [16], thus advancing health equity for social sustainability. The open-science approach further contributes to economic sustainability by fostering global partnerships and domestic innovations [33,34]. Consequently, the study reflects a practical paradigm shift toward equitable long-term prosperity for future generations.

In recent years, the landscape of restorative dentistry has evolved significantly with the application of additive manufacturing. One noteworthy development was the introduction of a filled resin by Bego, which was designed for vat photopolymerization to create definitive composite resin restorations. This product holds promise for printing with filled composites using established methods, with favorable outcomes in terms of marginal adaptation and biocompatibility [7,35]. However, importantly, the filler size of this product is similar to that of microfilled composites, and the filler content remains lower than that of most flowable composites [36]. Since microfilled composites with low filler contents may exhibit low wear resistance and poor mechanical properties, further studies are warranted to evaluate the in vitro and clinical performance of these novel materials [37,38].

In pursuit of restorations with improved wear resistance and mechanical properties, researchers have focused on the AM of zirconia ceramics and polymer-infiltrated ceramic network (PICN) composites

[1] "Perimeter" is defined as the outline of an outer surface or wall of a printed object. A printed object can have several perimeters. In the context of an occlusal surface, each cusp possesses a distinct perimeter. The term "stringing" refers to material being pulled from the printed area, forming a thin string. When the extruder moves from one cusp to the next, "perimeter crossing" may cause "stringing".

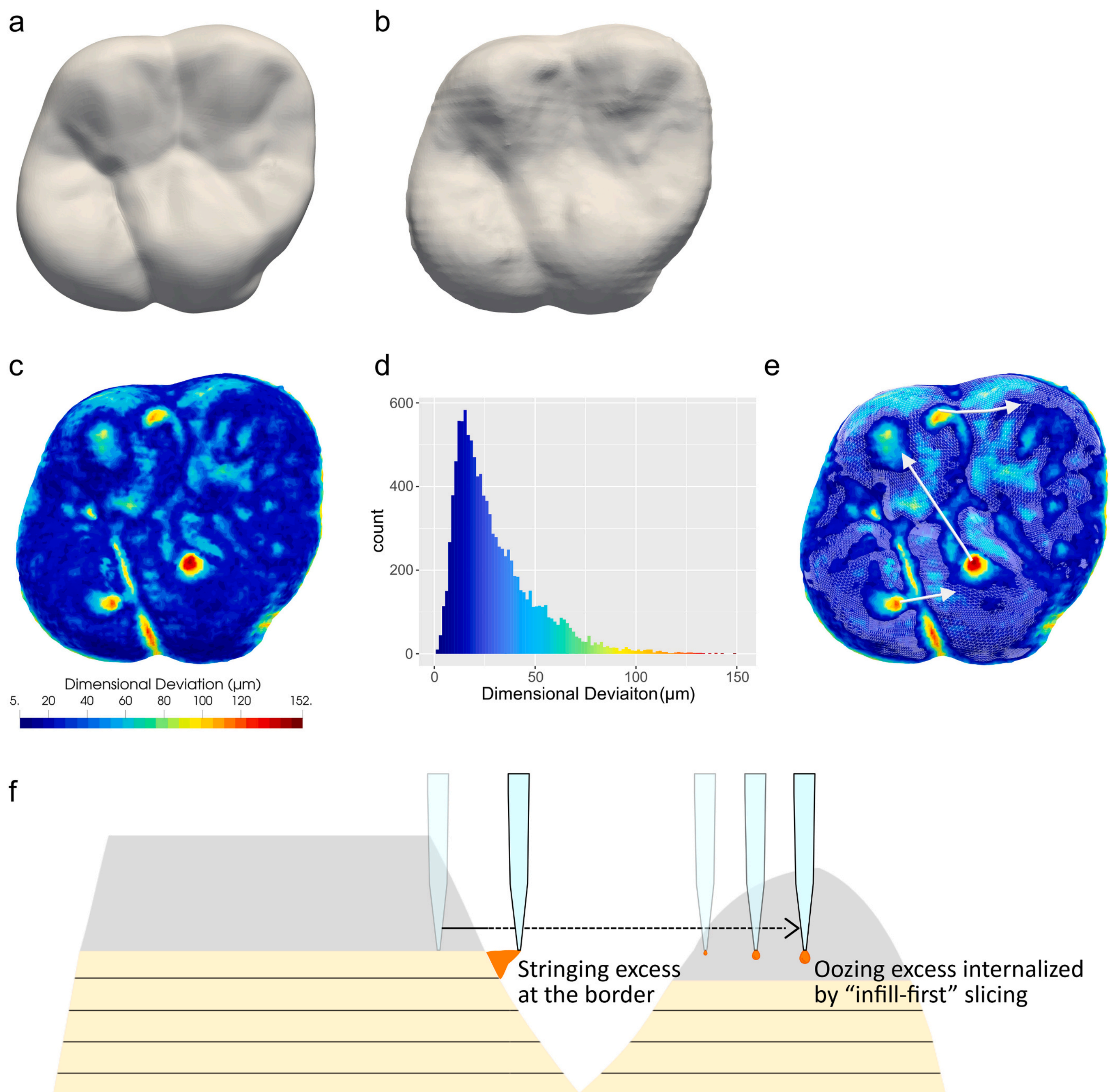

Fig. 4. Reference model and the dimensional deviation of a representative printed object. (a) Reference model. (b) Surface reconstructed from the point cloud of a representative sample. (c) Color map of the representative sample, illustrating its dimensional deviation from the reference model. (d) Deviation histogram of the representative sample. (e) Deviation map with the superimposed reference model shown as a white mesh. Areas without mesh indicate an excess amount of material. Additionally, nonextruding printing paths (white solid lines) imported from the G-codes are used to elucidate the link between material stringing and high-deviation areas. (f) Schematic diagram illustrating the concepts of stringing and oozing. When the extruder leaves the printed region, the nozzle drags a trace amount of viscoplastic composite from the border, leading to an excess; this process is referred to as the stringing phenomenon (left). On the other hand, the residual hydrostatic pressure within the nozzle causes material to ooze during long nonextrusion movements (right). The dimensional deviation from the oozing effect is minimized by adopting an "infill-first" slicing strategy, which initiates the printing of new regions from the infill and internalizes the excess oozed material. The same color scale applies to (c), (d), and (e).

[39]. A recent publication reported a promising sub-100 µm surface deviation in stereolithographic-printed zirconia restorations [40]. However, importantly, the drying process required for these materials is energy-intensive and time-consuming, posing challenges for on-demand applications. In addition, vat photopolymerization techniques often result in substantial residual resin remnants, highlighting the necessity of an alternative approach to facilitate the clean and on-demand production of definitive restorations.

To overcome these limitations, we opted for a different approach using DIW with resin composites. Despite the use of serial rather than parallel production, our approach is a viable option for chairside applications because it eliminates the need for time-consuming post-processing [40]. While prior studies employed the DIW technique to print resin-based tooth-like structures, the clinical relevance of this technique was limited; notably, the structures were printed with experimental hydroxyapatite resin composites, and the reported dimensional accuracy has yet to reach a clinically acceptable level [41, 42]. Thus, our primary objective was to investigate the feasibility of using DIW technology to produce resin composites in a clinically relevant context.

In our study, multiple accuracy metrics are used to fully assess the capability of the novel printing system (Table 1). The largest values were reported by the RMS, as it gives greater weight to larger values in the input data than do other metrics. Although commonly used to assess accuracy, the RMS calculation incorporates both variance and arithmetic mean components [43]. On the other hand, medians yield the smallest value in a right-skewed distribution, as extreme values have limited effects. Considering the nonnormal nature of an unsigned deviation, the median emerges as a suitable descriptor for trueness in this study. The observed differences among the trueness metrics indicate the need for more standardized statistics to enhance comparability among 3D printing studies [26].

Studies of digital manufacturing techniques often focus on trueness evaluation without reporting precision metrics [6,10,27,40,44]. By definition, precision reflects the agreement between independent test results or samples. As the variability statistics of the pooled deviation data reflect the variability in trueness across all sample points, they do not strictly represent precision [26]. To exclude within-sample trueness variability from calculations, pairwise superimposition is commonly employed to illustrate differences in individual pairs of scans [26]. However, pairwise operations generate numerous superimposition maps, posing challenges to implementation and subsequent outcome visualization. There is a need for an intuitive way to compute multi-sample precision and visualize the corresponding results in 3D to enhance the reliability of digital technologies in restorative dentistry.

In addition to the differences in trueness metrics, the effects of data aggregation on variability statistics are considered in this study. As shown in Table 1, the variability values of the overall trueness metrics consistently surpass those of the corresponding sample-specific metrics. From a statistical perspective, sample-specific metrics are based on aggregated data, where each sample is represented by its RMS, mean, and median deviation. While aggregation preprocessing serves to provide a concise overview of complex multilevel data, low-level variations are discarded, resulting in considerably smaller dispersion values.

Drawing an analogy to economics, the gross domestic product (GDP) per capita represents an aggregated value of produced goods and services divided by a country's average population. This definition is used to effectively highlight differences at the country level but overlooks variations among individual residents. Similarly, in studies of dimensional deviation, presenting statistics based on sample-specific trueness metrics offers insights into aggregated values at the sample level but fails to capture variability in within-sample deviations.

To illustrate the within-sample variability, an "overall" histogram and corresponding statistics derived from pooled surface-wide deviation data for all samples are obtained (Fig. 3b). This approach retains within-sample spatial variability, facilitating efficient parameter fine-tuning for accurate shapes. Specifically, the positively skewed distribution of the overall histogram suggests that only a small portion of the surface is characterized by a high deviation. A meticulous examination of the deviation maps was further performed to identify the high-deviation regions, which were protuberances caused by material excess. Statistical analysis was integrated with spatial visualization to optimize the printing accuracy. By overlaying the nonextrusion movements of the extruder onto the representative deviation map (Fig. 4e), we established the connection between the region of excess material and material stringing. This workflow not only enhances our understanding of dimensional deviations but also offers valuable insights for improving the printing accuracy.

Stringing, a broadly recognized phenomenon in extrusion-based 3D printing, is often confused with the term "oozing" in the 3D printing community. While both terms are associated with undesired material excess, it is crucial to delineate their distinctions to achieve high-accuracy printing. Oozing is an overextrusion resulting from the release of accumulated internal hydrostatic pressure [45]. This phenomenon tends to be prominent after nonextrusive movements. On the other hand, stringing is caused by the outward pulling of viscous materials and predominantly occurs as the extruder departs from the border of the printed region (also referred to as the perimeter) and moves toward the next printing region.

In this study, we alleviated the oozing problem by implementing an "infill-first" slicing strategy. In infill-first slicing, the extruder is directed to the inner part of the next printing region immediately after completing printing in the previous region; thus, the oozed excess is internally contained, and the deviation resulting from oozing is minimized. In contrast, managing the stringing phenomenon is more challenging because it is primarily affected by the viscosity of the material. Nevertheless, small regions of excess can be readily identified and corrected by clinicians. Moreover, optimizing the printing paths to reduce the number of perimeter-crossing events is a potential solution for the stringing problem [46].

The current study demonstrated the potential of DIW technology for use in the production of permanent composite resin restorations. Our findings suggest that the DIW system is well suited for clinical applications in restorative dentistry. However, importantly, while the flowable composite used in this study can be used for class II cavities, composites with higher filler loads are generally preferred due to their superior mechanical properties [47]. To fully leverage the potential of DIW technology, ongoing research should focus on assessing the compatibility of the system with hybrid and universal composites.

Despite the promising results of this study, there are still aspects that require further investigation. First, to assess the performance of DIW printers, a comparative analysis with other manufacturing systems should be performed. This approach would provide a better understanding of the advantages and limitations of DIW in relation to existing technologies. Second, the integration of an additional extruder is recommended, as many restorations include unsupported parts that necessitate support from sacrificial structures. Finally, future research should aim to expand the scope of application by exploring the printing of various types of fixed prostheses and assessing their fitness. Addressing these questions will further enhance the potential of using DIW technology in restorative dentistry.

The accuracy of manufacturing depends on various factors, such as the technology, printer specifications, materials used, geometries, and specific region of interest. In addition, studies have noted the effects of printing parameters on dimensional accuracy [48]. Meaningful comparisons of the accuracy values across different publications can be achieved only after taking these factors into account. To facilitate effective communication and comparison, establishing a consensus regarding standardized print geometry and statistics would be highly advantageous [26]. These benchmarks provide a foundation for future studies, enabling a more systematic approach to evaluating the accuracy of 3D printing technologies.

In conclusion, our study demonstrated the potential of using DIW technology in the on-demand production of indirect composite restorations. The analysis indicated that the proposed DIW system can achieve a dimensional accuracy comparable to that of the current subtractive manufacturing systems [6,40]. Based on its multifaceted support of sustainability and the dimensional accuracy demonstrated, the proposed DIW approach should be further researched and improved.

Declaration of Generative AI and AI-assisted technologies in the writing process

Statement: During the preparation of this work the authors used ChatGPT, an artificial intelligence (AI) language model developed by OpenAI, in order to improve the language of this manuscript. After using this service, the authors reviewed and edited the content as needed and take full responsibility for the content of the publication.

Acknowledgments

The authors would like to thank Mr. S. Ratzesberger for his initial work on the project, Mr. T. Obermeier for providing technical support and inspiration, and Mrs. G. Dachs and Mrs. E. Koebele for their efforts.

We would like to express sincere gratitude to Mr. Dipl.-Ing. Georg Hiebl, Syndicad Ingenieurbüro, Munich, Germany, for his support of this project, as he was constantly available to address any issues. Over the past 25 years of collaborative development of specialized dental testing machines, we have gained extensive knowledge in construction, mechanics, electronics, and programming. This collective experience enabled us to achieve the successful implementation of this project.

This project was partially funded by the DAAD, Germany (funding program 57507871 awarded to Po-Chun Tseng), and the Department of Conservative Dentistry and Periodontology, Ludwig-Maximilians-University of Munich, Germany. This study was also supported by a grant from the German Society of Restorative and Regenerative Dentistry (DGR^{2}Z) and Kulzer. Furthermore, we acknowledge the support provided by the IADR Kulzer Travel Award and the travel grant from the Taiwan Association for Dental Sciences, which facilitated our participation in the 2023 IADR/LAR General Session.

References

[1] Mehta SB, Lima VP, Bronkhorst EM, Crins L, Bronkhorst H, Opdam NJM, et al. Clinical performance of direct composite resin restorations in a full mouth rehabilitation for patients with severe tooth wear: 5.5-year results. J Dent 2021; 112:103743. https://doi.org/10.1016/j.jdent.2021.103743.

[2] Loomans BAC, Kreulen CM, Huijs-Visser H, Sterenborg B, Bronkhorst EM, Huysmans M, et al. Clinical performance of full rehabilitations with direct composite in severe tooth wear patients: 3.5 Years results. J Dent 2018;70:97–103. https://doi.org/10.1016/j.jdent.2018.01.001.

[3] Angeletaki F, Gkogkos A, Papazoglou E, Kloukos D. Direct versus indirect inlay/onlay composite restorations in posterior teeth. A systematic review and meta-analysis. J Dent 2016;53:12–21. https://doi.org/10.1016/j.jdent.2016.07.011.

[4] Tseng P-C, Chuang S-F, Kaisarly D, Kunzelmann K-H. Simulating the shrinkage-induced interfacial damage around Class I composite resin restorations with damage mechanics. Dent Mater 2023;39:513–21. https://doi.org/10.1016/j.dental.2023.03.020.

[5] Hayashi J, Shimada Y, Tagami J, Sumi Y, Sadr A. Real-Time Imaging of Gap Progress during and after Composite Polymerization. J Dent Res 2017;96:992–8. https://doi.org/10.1177/0022034517709005.

[6] Al Hamad KQ, Al Rashdan RB, Al Rashdan BA, Al Quran FA. Effect of CAD-CAM tool deterioration on the trueness of ceramic restorations. J Prosthet Dent 2022; 127:635–44. https://doi.org/10.1016/j.prosdent.2020.09.035.

[7] Daher R, Ardu S, di Bella E, Krejci I, Duc O. Efficiency of 3D-printed composite resin restorations compared with subtractive materials: evaluation of fatigue behavior, cost, and time of production. S0022391322004814 J Prosthet Dent 2022. https://doi.org/10.1016/j.prosdent.2022.08.001.

[8] Hegedus T, Kreuter P, Kismarczi-Antalffy AA, Demeter T, Banyai D, Vegh A, et al. User experience and sustainability of 3d printing in dentistry. Int J Environ Res Public Health 2022;19:1921. https://doi.org/10.3390/ijerph19041921.

[9] Andjela L, Abdurahmanovich VM, Vladimirovna SN, Mikhailovna GI, Yurievich DD, Alekseevna MY. A review on Vat Photopolymerization 3D-printing processes for dental application. Dent Mater 2022;38:e284–96. https://doi.org/10.1016/j.dental.2022.09.005.

[10] Lin C-H, Lin Y-M, Lai Y-L, Lee S-Y. Mechanical properties, accuracy, and cytotoxicity of UV-polymerized 3D printing resins composed of Bis-EMA, UDMA, and TEGDMA. J Prosthet Dent 2020;123:349–54. https://doi.org/10.1016/j.prosdent.2019.05.002.

[11] Rodríguez-Hernández AG, Chiodoni A, Bocchini S, Vazquez-Duhalt R. 3D printer waste, a new source of nanoplastic pollutants. Environ Pollut 2020;267:115609. https://doi.org/10.1016/j.envpol.2020.115609.

[12] Felici G, Lachowicz JI, Milia S, Cannizzaro E, Cirrincione L, Congiu T, et al. A pilot study of occupational exposure to ultrafine particles during 3D printing in research laboratories. Front Public Health 2023;11:1144475. https://doi.org/10.3389/fpubh.2023.1144475.

[13] Walpitagama M, Carve M, Douek AM, Trestrail C, Bai Y, Kaslin J, et al. Additives migrating from 3D-printed plastic induce developmental toxicity and neuro-behavioural alterations in early life zebrafish (Danio rerio). Aquat Toxicol 2019; 213:105227. https://doi.org/10.1016/j.aquatox.2019.105227.

[14] Saadi MASR, Maguire A, Pottackal NT, Thakur MSH, Ikram MMd, Hart AJ, et al. Direct ink writing: a 3d printing technology for diverse materials. Adv Mater 2022; 34:2108855. https://doi.org/10.1002/adma.202108855.

[15] Rocha VG, Saiz E, Tirichenko IS, García-Tuñón E. Direct ink writing advances in multi-material structures for a sustainable future. J Mater Chem A 2020;8: 15646–57. https://doi.org/10.1039/D0TA04181E.

[16] Teegen I-S, Schadte P, Wille S, Adelung R, Siebert L, Kern M. Comparison of properties and cost efficiency of zirconia processed by DIW printing, casting and CAD/CAM-milling. Dent Mater 2023;39:669–76. https://doi.org/10.1016/j.dental.2023.05.001.

[17] Cesarano III J., Calvert P. Freeforming objects with low-binder slurry. 20015682, 2000.

[18] Vatani M, Choi J-W. Direct-print photopolymerization for 3D printing. Rapid Prototyp J 2017;23:337–43. https://doi.org/10.1108/RPJ-11-2015-0172.

[19] Farahani RD, Lebel LL, Therriault D. Processing parameters investigation for the fabrication of self-supported and freeform polymeric microstructures using ultraviolet-assisted three-dimensional printing. J Micromech Microeng 2014;24: 055020. https://doi.org/10.1088/0960-1317/24/5/055020.

[20] Foster ED, Deardorff A. Open Science Framework (OSF). J Med Libr Assoc JMLA 2017;105:203–6. https://doi.org/10.5195/jmla.2017.88.

[21] Peek N, Moyer I. Popfab: A case for portable digital fabrication. Proc. Elev. Int. Conf. Tangible Embed. Embodied Interact. Yokohama Japan: ACM,; 2017. p. 325–9. https://doi.org/10.1145/3024969.3025009.

[22] Al Sunbul H, Silikas N, Watts DC. Polymerization shrinkage kinetics and shrinkage-stress in dental resin-composites. Dent Mater 2016;32:998–1006. https://doi.org/10.1016/j.dental.2016.05.006.

[23] Besl PJ, McKay ND. A method for registration of 3-D shapes. IEEE Trans Pattern Anal Mach Intell 1992;14:239–56. https://doi.org/10.1109/34.121791.

[24] Marcel R, Reinhard H, Andreas K. Accuracy of CAD/CAM-fabricated bite splints: milling vs 3D printing. Clin Oral Invest 2020;24:4607–15. https://doi.org/10.1007/s00784-020-03329-x.

[25] Mehl A, Gloger W, Kunzelmann K-H, Hickel R. A new optical 3-d device for the detection of wear. J Dent Res 1997;76:1799–807. https://doi.org/10.1177/00220345970760111201.

[26] Mehl A, Reich S, Beuer F, Güth J-F. Accuracy, trueness, and precision - a guideline for the evaluation of these basic values in digital dentistry. Int J Comput Dent 2021;24:341–52.

[27] Bae E-J, Jeong I-D, Kim W-C, Kim J-H. A comparative study of additive and subtractive manufacturing for dental restorations. J Prosthet Dent 2017;118: 187–93. https://doi.org/10.1016/j.prosdent.2016.11.004.

[28] Hickel R, Brüshaver K, Ilie N. Repair of restorations – Criteria for decision making and clinical recommendations. Dent Mater 2013;29:28–50. https://doi.org/10.1016/j.dental.2012.07.006.

[29] Spijker A, Rodriguez J, Kreulen C, Bronkhorst E, Bartlett D, Creugers N. Prevalence of tooth wear in adults. Int J Prosthodont 2009;22:35–42.

[30] United Nations. Department of Economic and Social Affairs. The Sustainable Development Goals: Report 2022. UN; 2022.

[31] Duane B, Stancliffe R, Miller F, Sherman J, Pasdeki-Clewer E. Sustainability in dentistry: a multifaceted approach needed. 002203452091939 J Dent Res 2020;99. https://doi.org/10.1177/0022034520919391.

[32] Duane B., editor. Sustainable Dentistry: Making a Difference. Cham: Springer International Publishing; 2022. https://doi.org/10.1007/978-3-031-07999-3.

[33] Burgelman J-C, Pascu C, Szkuta K, Von Schomberg R, Karalopoulos A, Repanas K, et al. Open science, open data, and open scholarship: european policies to make science fit for the twenty-first century. Front Big Data 2019;2:43. https://doi.org/10.3389/fdata.2019.00043.

[34] Govaart GH, Hofmann SM, Medawar E. The sustainability argument for open science. Collabra Psychol 2022;8:35903. https://doi.org/10.1525/collabra.35903.

[35] Wuersching SN, Hickel R, Edelhoff D, Kollmuss M. Initial biocompatibility of novel resins for 3D printed fixed dental prostheses. Dent Mater 2022;38:1587–97. https://doi.org/10.1016/j.dental.2022.08.001.

[36] Grzebieluch W, Kowalewski P, Grygier D, Rutkowska-Gorczyca M, Kozakiewicz M, Jurczyszyn K. Printable and machinable dental restorative composites for CAD/CAM application—comparison of mechanical properties, fractographic, texture and fractal dimension analysis. Materials 2021;14:4919. https://doi.org/10.3390/ma14174919.

[37] Lim BS, Ferracane JL, Condon JR, Adey JD. Effect of filler fraction and filler surface treatment on wear of microfilled composites. Dent Mater 2002;18:1–11. https://doi.org/10.1016/s0109-5641(00)00103-2.

[38] Prause E, Malgaj T, Kocjan A, Beuer F, Hey J, Jevnikar P, et al. Mechanical properties of 3D-printed and milled composite resins for definitive restorations: an in vitro comparison of initial strength and fatigue behavior. J Esthet Restor Dent 2024;36:391–401. https://doi.org/10.1111/jerd.13132.

[39] Sodeyama MK, Ikeda H, Nagamatsu Y, Masaki C, Hosokawa R, Shimizu H. Printable PICN composite mechanically compatible with human teeth. J Dent Res 2021;100:1475–81. https://doi.org/10.1177/00220345211012930.

[40] Lüchtenborg J, Willems E, Zhang F, Wesemann C, Weiss F, Nold J, et al. Accuracy of additively manufactured zirconia four-unit fixed dental prostheses fabricated by stereolithography, digital light processing and material jetting compared with subtractive manufacturing. Dent Mater 2022;38:1459–69. https://doi.org/10.1016/j.dental.2022.06.026.

[41] Zhao M, Geng Y, Fan S, Yao X, Zhu M, Zhang Y. 3D-printed strong hybrid materials with low shrinkage for dental restoration. Compos Sci Technol 2021;213:108902. https://doi.org/10.1016/j.compscitech.2021.108902.

[42] Zhao M, Yang D, Fan S, Yao X, Wang J, Zhu M, et al. 3D-printed strong dental crown with multi-scale ordered architecture, high-precision, and bioactivity. Adv Sci 2022;9:2104001. https://doi.org/10.1002/advs.202104001.

[43] Deakin RE, Kildea DG. A note on standard deviation and RMS. Aust Surv 1999;44: 74–9. https://doi.org/10.1080/00050351.1999.10558776.

[44] Park J-M, Jeon J, Koak J-Y, Kim S-K, Heo S-J. Dimensional accuracy and surface characteristics of 3D-printed dental casts. J Prosthet Dent 2021;126:427–37. https://doi.org/10.1016/j.prosdent.2020.07.008.

[45] Greeff GP, Schilling M. Single print optimisation of fused filament fabrication parameters. Int J Adv Manuf Technol 2018;99:845–58. https://doi.org/10.1007/s00170-018-2518-4.

[46] Kaplan D, Rorberg S, Ben Chen M, Sterman Y. NozMod: Nozzle modification for efficient FDM 3d printing. Proc. 7th Annu. ACM Symp. Comput. Fabr., Seattle WA USA: ACM. 2022. p. 1–9. https://doi.org/10.1145/3559400.3561999.

[47] Lohbauer U, Belli R, Ferracane JL. Factors involved in mechanical fatigue degradation of dental resin composites. J Dent Res 2013;92:584–91. https://doi.org/10.1177/0022034513490734.

[48] Piedra-Cascón W, Krishnamurthy VR, Att W, Revilla-León M. 3D printing parameters, supporting structures, slicing, and post-processing procedures of vat-polymerization additive manufacturing technologies: a narrative review. J Dent 2021;109:103630. https://doi.org/10.1016/j.jdent.2021.103630.